Conformation and Dynamics of Membrane-Bound Digalactosyldiacylglycerol†

Kathleen P. Howard‡ and James H. Prestegard*

Contribution from the Department of Chemistry, Yale University, New Haven, Connecticut 06520

Received August 28, 1995. Revised Manuscript Received January 16, 1996⊗

Abstract: The conformation and dynamics of a uniformly ^{13}C-labeled glycolipid, digalactosyldiacylglycerol (DGDG), is studied in a membrane environment using NMR spectroscopy. Dipolar couplings and ^{13}C chemical shift anisotropy offsets which appear in magnetically oriented phospholipid-based membrane fragments are used to derive a detailed description of the conformation and amplitudes of motion. ^{13}C relaxation rates (T_1, T_2, and NOE) were then measured for ^{13}C sites in DGDG anchored to isotropically tumbling phospholipid bilayers. Using a Lipari and Szabo type approach, a nonlinear least squares fit of relaxation rates to motional parameters yielded rates and amplitudes of internal motions for the first and terminal sugar of the glycolipid head group. Generalized order parameters extracted from relaxation data show good agreement with order parameters used to fit dipolar couplings. The combined model is analyzed in terms of potential energy maps generated using a version of AMBER modified to include a membrane interaction energy term. The experimental conformational preferences of the terminal α(1−6) linkage in DGDG agree quite well with predictions based on these calculations.

Introduction

Molecules anchored at cell surfaces are conveniently positioned to modulate communication between cells and their external environment by acting as receptors for a variety of physiologically and pathologically active agents. The oligosaccharide head groups of glycolipids, in particular, are known to serve as markers for cell differentiation and development[1] as well as receptors for viruses, bacteria and toxins.[2] The conformation and dynamics of glycolipids at a membrane surface are therefore of fundamental interest.

Unfortunately, studying glycolipids within a lipid lattice has presented serious obstacles for the application of the most widely used methods of structural biology. Membrane systems have proven difficult to crystallize for use in X-ray diffraction studies.[3] Solution state nuclear magnetic resonance (NMR) has been used to study membrane-bound glycolipids incorporated into small micelles or unilamellar vesicles,[4] but broad line widths and efficient spin diffusion that accompany the relatively slow reorientation of micelle complexes complicate structural analysis. An alternative approach employs solid state NMR techniques. These techniques have proven to be particularly useful in the study of membrane-bound phospholipids[5−7] and glycolipids,[8−10] but they are often limited by the need for isotopic enrichment of particular sites. Recently, we have developed methodology utilizing magnetically oriented phospholipid bilayers to study the conformation of membrane-bound molecules.[11] Under appropriate conditions of concentration and magnetic field strength, discoidal fragments of phospholipid bilayers orient in a way that retains a portion of the dipolar splittings and chemical shift anisotropy offsets seen in solid state NMR. Orientational constraints derived from dipolar and quadrupolar couplings and chemical shift anisotropy (CSA) data parallel those obtained with solid state NMR techniques, but resolution is retained to a point where uniform labeling can be considered.

Diacylglycerol glycolipids are a class of glycolipids that occur widely in nature as components of the chloroplast membranes of higher plants and the cell membranes of prokaryotic blue-green algae.[12] The two most abundant diacylglycerols are monogalactosyldiacylglycerol (MGDG) and digalactosyldiacylglycerol (DGDG). Although their particular roles are unknown, it has been proposed that MGDG and DGDG stabilize and help determine the shape of chloroplast membranes, as well as play a role in the insertion and stabilization of the large photosystem protein complexes.[12,13]

We recently reported a detailed NMR study of uniformly ^{13}C-labeled MGDG.[14] Analysis of the membrane-bound conformation of MGDG was based on measurement of dipolar interactions between sites on the head group, as well as between sites on the backbone, and on the measurement of ^{13}C chemical shift anisotropy offsets which appear in magnetically oriented phospholipid-based membrane bilayers. Here we extend the methodology to treat DGDG. Like MGDG, the head group of DGDG consists of a galactose linked in a β-configuration to a glycerol backbone. The second galactose of DGDG is attached by a α(1−6) linkage (see Figure 1). The (1−6) linkage involves

* To whom correspondence should be addressed.

† This work was supported by the National Institutes of Health Grant GM33225.

‡ Present address: Department of Chemistry, University of Pennsylvania, Philadelphia, PA 19104.

⊗ Abstract published in *Advance ACS Abstracts,* March 15, 1996.

(1) Hakomori, S. *Curr. Opin. Immunol.* **1991**, *3*, 646−653.
(2) Weiss, W.; Brown, J.; Cusack, S.; Paulson, J.; Skehel, J.; Wiley, D. *Nature* **1988**, *333*, 426−431.
(3) Pascher, I.; Lundmark, M.; Nyholm, P.; Sundell, S. *Biochim. Biophys. Acta* **1992**, *1113*, 339−373.
(4) Siebert, H.; Reuter, G.; Schauer, R.; von der Lieth, C.; Dabrowski, J. *Biochemistry* **1992**, *31*, 6962−6971.
(5) Smith, S. O.; Kustanovich, I.; Bhamidipati, S.; Salmon, A.; Hamilton, J. A. *Biochemistry* **1992**, *31*, 11660−11664.
(6) Strenk, L. M.; Westerman, P. W.; Doane, J. W. *Biophys. J.* **1985**, *48*, 765−773.
(7) Braach-Maksvytis, V. L. B.; Cornell, B. A. *Biophys. J.* **1988**, *53*, 839−843.
(8) Jarrell, H.; Jovall, P.; Giziewicz, J.; Turner, L.; ICP, S. *Biophys. J.* **1987**, *63*, 428−437.
(9) Auger, M.; Van Calsteren, M.; Smith, I.; Jarrell, H. *Biochemistry* **1990**, *29*, 5815−5821.
(10) Skarjune, R.; Oldfield, E. *Biochemistry* **1982**, *21*, 3154−3160.
(11) Sanders, C.; Hare, B.; Howard, K.; Prestegard, J. *Prog. NMR Spectrosc.* **1994**, *26*, 421−444.
(12) Curatolo, W. *Biochim. Biophys. Acta* **1987**, *906*, 137−160.
(13) Quinn, P.; Williams, W. *Biochim. Biophys. Acta* **1983**, *737*, 223−266.
(14) Howard, K.; Prestegard, J. *J. Am. Chem. Soc.* **1995**, *117*, 5031−5040.

0002-7863/96/1518-3345$12.00/0

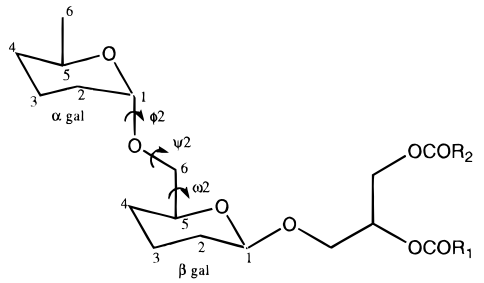

Figure 1. Structure of DGDG. R is $(CH_2)_nCH_3$.

three conformationally labile linkage bonds, whereas the more common (1−4) and (1−3) linkages between sugars involve only two. The additional degree of freedom results in (1−6) linkages being among the most flexible of glycosidic links.[15] The presence of two sugars in uniformly labeled DGDG also affords an opportunity to test resolution limitations of the oriented phase methodology. Previous studies in magnetically oriented membranes, including the MGDG study mentioned above, have focused on the conformation of a single isotopically labeled carbohydrate residue in a glycolipid.[16−18]

In addition to conformational preferences of the carbohydrate head group, we were able to study the dynamics of the glycosidic linkages in DGDG. ^{13}C T_1's, T_2's, and heteronuclear NOEs were measured for the two anomeric carbons of membrane-bound DGDG and are used to estimate relative time scales and amplitudes of motions for the two galactose residues. Analysis of both dipolar coupling data and relaxation rates yield order parameters. Values produced by the two methods can be compared.

The dynamic studies of DGDG presented here are of particular interest, not only due to a lack of data on the flexibility of glycosidic linkages in the literature but also because the experiments are carried out in the physiologically relevant environment of a membrane interface. ^{13}C relaxation studies have been applied to many small oligosaccharides in solution.[19,20] However, for small oligosaccharides where internal motion is on the order of the overall molecular tumbling, it is difficult to separate internal and overall motion on the basis of time scales. Studying sugars attached to large micellar assemblies results in slow overall tumbling and allows separation of internal motion effects associated with the glycosidic linkages.[21,22] Comparisons can be made with previous studies of membrane-bound lipids using ^2H NMR.[9,23−26] ^{13}C relaxation experiments, as applied here, promise some additional insight because of the number of sites that can be observed and the variety of relaxation experiments that can be conducted. Finally, the data collected can be used to assess the viability of molecular modeling approaches to the description of conformational preferences of glycolipids at membrane surfaces. Potential energy maps for the α(1−6) linkage of DGDG were calculated as a function of the interglycosidic torsions $\phi 2$, $\psi 2$, and $\omega 2$ using a version of AMBER modified to include a membrane interaction energy.[27,28] The calculated minimum energy structures agree quite well with experimental data.

Materials and Methods

Materials. 3-[(Cholamidopropyl)dimethylammonio]-2-hydroxyl-1-propanesulfonate (CHAPSO) and L-α-dimyristoylphosphatidylcholine (DMPC) were purchased from Sigma Chemical Co. (St. Louis, MO). Uniformly ^{13}C (∼26% and ∼98%) labeled algal extracts were obtained from Cambridge Isotopes (Andover, MA), and ^{13}C-labeled DGDG was isolated from these algal extracts using flash chromatography on a series of silica gel columns. Elution was with 13:7:1 chloroform/methanol/ammonium hydroxide) and 91:30:6:2 (acetone/toluene/water/acetic acid.[29] All reagents used in the purification of DGDG or the preparation of NMR samples were purchased from either Sigma Chemical Co. (St. Louis, MO) or Aldrich Chemical Co. (Milwaukee, WI).

Preparation of NMR Samples. Liquid crystalline NMR samples, comprised of arrays of bilayer disks, were prepared directly in 5 mm NMR tubes. A complete description of the oriented DMPC/CHAPSO system has been published elsewhere.[11,30] Briefly, ∼10 mg of ^{13}C-labeled DGDG, 107 mg of DMPC, and 33 mg of CHAPSO were mixed in 350 μL of buffer (0.1 M NaCl, 1 mM DTT, 50% D_2O, 50% H_2O) by a combination of centrifugation, heating, cooling, and sonication until a homogeneous sample was obtained. The samples intended for magnetically induced orientation had a lipid content of 30%. Samples were diluted to a lipid content of 20% to induce isotropic tumbling for the determination of the signs of dipolar couplings and the measurement of relaxation times.

NMR Spectroscopy. Solution spectra were collected on either a Bruker AM-500 spectrometer or a GE Omega 500 spectrometer (125.76 MHz for ^{13}C, 500 MHz ^1H). A ^1H double-quantum filtered correlation experiment (DQFCOSY)[31] was used to partially assign proton resonances of DGDG. A heteronuclear multiple quantum coherence experiment (HMQC)[32] and heteronuclear multiple bond coherence experiment (HMBC)[33] allowed correlation of ^1H and ^{13}C resonances and ultimately partial assignment of ^{13}C resonances. Severe overlap prevented full assignment using just these two-dimensional methods. Taking advantage of the ^{13}C enrichment, ^1H-detected three-dimensional ^{13}C single- and double-quantum COSY experiments allowed for full assignment of ^1H and ^{13}C resonances.[34] (^{13}C assignments for the head group of DGDG are reported in Chung et al.[34]) Assignments of carbon resonances of DGDG in the oriented membrane samples were based on analogy to solution data and reinforced by connectivities observed in the $^{13}C-^{13}C$ correlation experiments under oriented conditions.

All oriented spectra were collected unlocked and without sample spinning. ^1H-decoupled ^{31}P spectra for the estimation of $S_{bilayer}$ were collected on a GE Omega 300 spectrometer (121 MHz for ^{31}P). ^{13}C-oriented spectra were collected on a Bruker AM 500 using a standard 5 mm $^{13}C-^1H$ dual probe (^{13}C 90 pw ∼ 6.2 μs; ^1H 90 pw ∼ 26 μs). ^1H decoupling was effected using WALTZ[35] with maximum available (40 W) decoupling power only during acquisition. To avoid sample heating due to high decoupling levels, acquisition times were limited to about 40 ms with delays of approximately 1.5 s between acquisitions.

(15) Homans, S.; Edge, C.; Ferguson, M.; Dwek, R.; Rademacher, T. *Biochemistry* **1989**, *28*, 2881−2887.
(16) Aubin, Y.; Prestegard, J. *Biochemistry* **1993**, *32*, 3422−3428.
(17) Hare, B.; Rise, F.; Aubin, Y.; Prestegard, J. *Biochemistry* **1994**, *33*, 10137−10148.
(18) Sanders, C.; Prestegard, J. *J. Am. Chem. Soc.* **1992**, *114*, 7096−7107.
(19) Poppe, L.; van Halbeek, H. *J. Am. Chem. Soc.* **1992**, *114*, 1092−1094.
(20) McCain, D.; Markley, J. *J. Am. Chem. Soc.* **1986**, *108*, 4529−4264.
(21) Goux, W.; Perry, C.; James, T. *J. Biol. Chem.* **1982**, *257*, 1829−1835.
(22) Poppe, L.; van Halbeek, H.; Acquotti, D.; Sonnino, S. *Biophys. J.* **1994**, *66*, 1642−1652.
(23) Siminovitch, D.; Olejinczak, E.; Ruocco, M.; Das Gupta, S.; Griffin, R. *Chem. Phys.Lett.* **1985**, *119*, 251−255.
(24) Seelig, J. *Q. Rev. Biophys.* **1977**, *10*, 353−418.
(25) Smith, R.; Oldefield, E. *Science* **1984**, *225*, 280−288.
(26) Singh, D.; Shan, X.; Davis, J.; Jones, D.; Grant, C. *Biochemistry* **1995**, *34*, 451−463.
(27) Hare, B.; Howard, K.; Prestegard, J. *Biophys. J.* **1993**, *64*, 392−398.
(28) Ram, P.; Kim, E.; Thomson, D.; Howard, K.; Prestegard, J. *Biophys. J.* **1992**, *63*, 1530−1535.
(29) Sato, N.; Murata, N. *Methods Enzymol.* **1988**, *167*, 251−259.
(30) Sanders, C.; Prestegard, J. *Biophys. J.* **1990**, *58*, 447−460.
(31) Rance, M.; Sorensen, O.; Bodenhausen, G.; Wagner, G.; Ernst, R.; Wuthrich, K. *Biochem. Biophys. Res. Commun.* **1983**, *117*, 479−485.
(32) Bax, A.; Griffey, R.; Hawkins, B. *J. Mag. Reson.* **1983**, *55*, 301−315.
(33) Bax, A.; Summers, M. *J. Am. Chem. Soc.* **1986**, *108*, 2093−2094.
(34) Chung, J.; Tolman, J.; Howard, K.; Prestegard, J. *J. Magn. Reson.* **1993**, *102 B*, 137−147.
(35) Shaka, A.; Keeler, J.; Freeman, R. *J. Magn. Reson.* **1983**, *53*, 313−340.

For sensitivity enhancement through nuclear Overhauser effects (NOEs), ^{13}C spectra were collected with low-power (0.3 W) decoupling during the predelay. Spectral widths for ^{13}C spectra were commonly 25 000 Hz. Approximately 150 scans were needed to achieve a S/N ratio of 10/1 in a ^{1}H-decoupled ^{13}C spectrum (acquired with 0.3 W of decoupling during the predelay) of ~10 mg of 26% ^{13}C DGDG in 3:1 DMPC/CHAPSO at 305 K (7 mm ^{13}C). ^{13}C FIDs were generally collected with 1K points, zero filled to 2K points and then exponentially multiplied with 10 Hz line broadening (20 Hz line broadening for $^{13}C-^{1}H$ coupled spectra).

$^{13}C-^{13}C$ dipolar couplings for DGDG were measured using ^{1}H-decoupled $^{13}C-^{13}C$ double-quantum filtered correlation experiments, DQFCOSY,[31] and 2D INADEQUATE.[36] Severe overlap prevented all but the well-resolved C1 and C6 couplings from being resolved in a DQFCOSY spectrum of DGDG. However, a series of 2D INADEQUATE spectra optimized for $(J + D) = 150-300$ Hz provided resolution of enough couplings for conformational analysis. Peaks in the indirect dimension of a 2D INADEQUATE occur at a frequency which corresponds to the sum of the chemical shifts of coupled carbons which, along with the absence of diagonal peaks, leads to better resolution. For both DQFCOSY and 2D INADEQUATE experiments, 128 t_1 points were collected with approximately 1024 scans per experiment (at least 48 h total acquisition). The sweep widths were generally 26 000 Hz in t_2 and 8500 Hz in the t_1 dimension.

Relaxation experiments were carried out for 26% ^{13}C uniformly labeled DGDG in 20% w/v DMPC/CHAPSO (3:1) at 292 K (isotropic conditions). Performing relaxation experiments under these conditions allowed the study of DGDG in a membrane-bound environment, while maintaining overall isotropic tumbling of the membrane disks. This simplifies relaxation analysis. We focus here on ^{13}C relaxation times for the well-resolved anomeric position of each sugar. T_2 values were measured from the half-width of the Lorenztian line shape, $\nu_{1/2}$ ($T_2 = 1/\pi\nu_{1/2}$). T_1 relaxation times were measured using an inversion recovery sequence ($180-\tau-90$) in which proton decoupling was employed throughout. The π pulse was 11.8 μs, and the recycle delay was 12.5 s. 12τ values were collected with 896 scans each. Intensity changes were fit to a single exponential to extract a T_1 value. NOEs were measured from the ratio of the peak amplitudes of spectra in which proton decoupling was applied throughout, (0.3 W, then 40 W during acquisition) to those where high-power proton decoupling was applied during collection of the FID, but remained gated off for a period of 2 s before acquisition of successive FIDs.

Analysis of Anisotropic Spectral Parameters. Both dipolar couplings and chemical shift anisotropy offsets are a source of structural and dynamic information in anisotropic media. Dipolar couplings, $D_{i,j}$, may be written as follows:

$$D_{ij} = \frac{-\gamma_i\gamma_j h}{2\pi^2 r^3} S_{\text{system}} S_{\text{mol}} \overline{\left(\frac{3\cos^2\theta - 1}{2}\right)} \qquad (1)$$

where γ_i and γ_j are the gyromagnetic ratios of the two interacting nuclei, h is Planck's constant, r is the distance between coupled nuclei, and θ is the angle between a given internuclear vector $i-j$ and the bilayer normal.[37] Net orientation and motion of the bilayer discs that comprise the liquid crystalline assemblies is included in a single order parameter, S_{system}, that scales all spectral parameters. S_{system} is defined as

$$S_{\text{system}} = -{}^1/_2 S_{\text{bilayer}} \qquad (2)$$

where the factor of $-{}^1/_2$ arises from the fact that DMPC bilayer discs orient with their normals at about 90° relative to the field and rotate rapidly about this axis. The bilayer disks also wobble about the average orthogonal direction in an axially symmetric fashion. S_{bilayer} describes the residual order of the bilayer normal axes in comparison to a fully extended bilayer membrane. In our analysis S_{bilayer} is assigned a value of 0.51 based on the anisotropic ^{31}P shift of DMPC comprising the bulk of our lipid matrix, relative to the ^{31}P shift seen in multilayer dispersions. Over and above S_{system}, experimental splittings are reduced by local molecular motions relative to the bilayer normal. S_{mol} is an order parameter assigned to account for reduction of couplings due to axially symmetric motion of the membrane anchor of DGDG. Although the assumption of axially symmetric averaging is an oversimplification, the approximate cylindrical shape of DGDG suggests relatively unhindered rotation and oscillation about the most ordered director axis. Further motion about glycosidic torsion angles which can scale down dipolar couplings measured for the two galactose residues in the head group is included in the average implied by the bar over the angular term in eq 1. Two different methods were used to treat the averaging of the angular term, order matrix analysis and torsion angle analysis.[11] Torsion angle analysis[27] is used to find a description for the conformation and dynamics of DGDG in terms of glycosidic torsions and motional averaging about these torsions. The more general treatment of order matrix analysis can be used to fit the experimental dipolar couplings to an orientation of the molecular frame with respect to the bilayer normal and principle elements of an order matrix. Here we will assume axial symmetry, reducing this analysis to fitting an orientation and an axially symmetric order parameter. A full description of the analysis is provided in the Results.

Carbonyls at the ester linkages of DGDG have measurable chemical shift anisotropies, CSA, that can also provide useful conformational and dynamic information. The observed chemical shift in an anisotropic system shows a dependence on order and molecular orientation which is very similar to that for dipolar coupling described above.[11,14]

Molecular Modeling. Conformational energy maps as a function of the torsion angles of the interresidue linkage, ϕ_2 (O5α−C1α−O6β−C6β), ψ_2 (C1α−O6β−C6β−C5β), and ω_2 (O6β−C6β−C5β−C4β), were calculated. A starting structure for DGDG was obtained by linking a crystal structure for galactose[38] to the membrane-bound solution structure of MGDG as previously described.[14] Three families of starting structures were generated, one for each of the staggered conformations of ω_2. Within these, the ϕ_2 and ψ_2 torsion angles were rotated at 20° intervals to generate starting structures, using the MULTIC option of MacroModel V3.1.[39] Energy minimization was performed at each grid point to generate relaxed energy maps using a version of AMBER 4.0[40] modified to include a membrane interaction energy.[27,28] Minimization included all degrees of freedom except for the torsion angles defining the respective grid points. After 5000 cycles of steepest descent, conjugate gradient minimization was used to achieve a convergence criterion of 0.05 kcal/mol. A force field with improved parameterization for oligosaccharides was utilized.[41]

Results

Figure 2a is the $^{13}C-^{1}H$ decoupled spectrum of 26% ^{13}C-labeled DGDG dissolved in CD_3OD. The anomeric position of each ring is labeled. The 10 other saccharide resonances and three glycerol peaks are in the crowded region between 60 and 75 ppm. With the exception of some unsaturated sites near 130 ppm, most acyl chain resonances are far upfield (<40 ppm). Carbonyl resonances are near 175 ppm. Figure 2b is the $^{13}C-^{1}H$ decoupled spectrum of 26% ^{13}C-labeled DGDG reconstituted into the DMPC/CHAPSO model membrane system under conditions where magnetic orientation is achieved (30% w/v DMPC/CHAPSO (3:1) at 305 K). When incorporated into the membrane discs, the ^{13}C resonances from DGDG broaden and become partially obscured by the natural abundance ^{13}C signal from the membrane matrix. The two anomeric positions remain well-resolved but adopt distinctly different line widths. The anomeric carbon of the β-linked galactose closest to the membrane is broad (140 Hz). The anomeric resonance from the second α-linked sugar is much sharper (50 Hz). The sugar/

(36) Mareci, T.; Freeman, R. *J. Magn. Reson.* **1982**, *48*, 158−163.
(37) Harris, R. *Nuclear Magnetic Resonance Spectroscopy*; John Wiley & Sons, Inc.: New York, 1983; p 260.
(38) Takagi, S.; Jeffrey, G. A. *Acta Crystallogr.* **1978**, *B*, 2006−2010.
(39) Still, W. C. *MacroModel V3.1*; Department of Chemistry, Columbia University: New York, 1990.
(40) Pearlman, D. A.; Case, D. A.; Caldwell, J. C.; Seibel, G. L.; Singh, C.; Weiner, P.; Kollman, P. A. *AMBER 4.0*; University of California: San Franicisco, CA, 1991; pp
(41) Scarsdale, J. N.; Ram, P.; Prestegard, J. H. *J. Comput. Chem.* **1988**, *9*, 133−147.

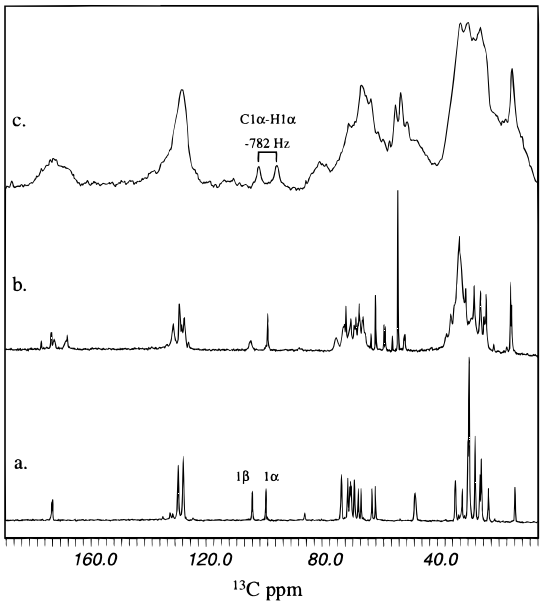

Figure 2. (a) ^{13}C−^{1}H decoupled spectrum of 26% ^{13}C DGDG in CD_3OD at 303 K. (b) ^{13}C−^{1}H decoupled spectrum of 26% ^{13}C DGDG in 30% w/v DMPC/CHAPSO (3:1) at 305 K. (c) ^{13}C−^{1}H coupled spectrum of the same sample as in b.

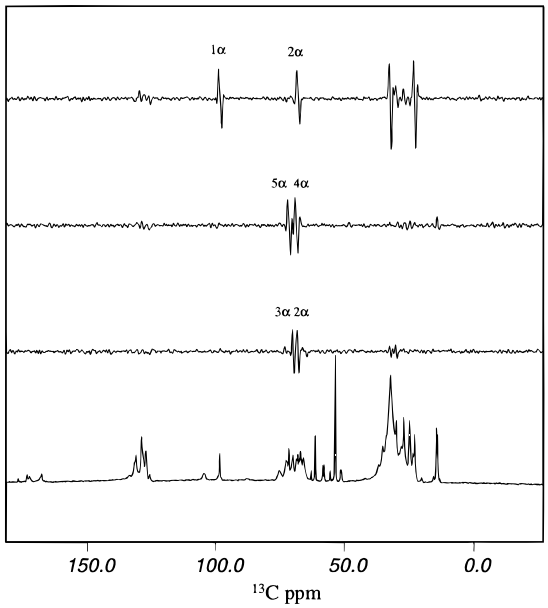

Figure 3. D_2 slices from a 2D INADEQUATE (125.76 MHz) optimized for $(J + D) = 150$ Hz. The spectrum was processed using sinebell multiplication in both dimensions.

glycerol region in Figure 2b is composed of a series of sharp peaks from the α-linked galactose superimposed on a series of broad peaks arising from the β-linked galactose. The carbonyl region now has five peaks; one from CHAPSO (177.5 ppm), two sharp peaks from the DMPC carbonyls (175 and 168 ppm), and two broad peaks from the DGDG carbonyls (173 and 169 ppm). Comparing Figure 2b with the same sample under isotropic conditions (not shown) permits the measurement of the CSA offsets. The CSA offsets for the β and γ chain carbonyls of DGDG are -5.0 ± 1.2 and -2.1 ± 1.2 ppm, respectively. This is very similar to the CSA offsets measured for the carbonyl resonances in MGDG (-5.1 ± 1.2 and -1.2 ± 1.2 ppm).[14]

Measurement of Dipolar Couplings for the α-Linked Galactose. Interference from peaks from isolated ^{13}C sites from DGDG and from natural abundance sites in the supporting membrane matrix prevents measurement of dipolar ^{13}C−^{13}C couplings directly from Figure 2b. However, as depicted in Figure 2c, the ^{1}H-coupled version of Figure 2b allows clear resolution of the C1α−H1α coupling (−782 Hz). The sign of the C1α−H1α dipolar coupling was determined from the temperature dependence of the C1α−H1α splitting in a series of 1D ^{1}H-coupled ^{13}C spectra of 26% ^{13}C DGDG in 20% w/v DMPC/CHAPSO (3:1). As the temperature is decreased from 305 to 292 K, the sample gradually looses its orientation and becomes isotropic. As this occurs, the C−H coupling passes through a minimum and then splits to reach a 150 Hz purely scalar coupling at 292 K.[11] This suggests that dipolar and scalar contributions to the splitting are of opposite sign, yielding a negative value for the C1α−H1α dipolar coupling.

^{13}C−^{13}C dipolar couplings were measured from series of 2D INADEQUATE spectra optimized for $(J + D) = 150-300$ Hz. D_2 slices from a 2D INADEQUATE optimized for $J = 150$ are shown in Figure 3. Three couplings, all from the second α-linked galactose are shown. The sign of C1α−C2α was determined to be positive from the temperature dependence of the C1α−C2α splitting in a series of 1D ^{1}H-decoupled ^{13}C spectra of 98% ^{13}C DGDG in 20% w/v DMPC/CHAPSO (3:1). The C4α−C5α internuclear vector is nearly parallel to C1α−C2α and was assigned a positive sign as well. The dipolar coupling data for the α-linked galactose are summarized in Table 1.

Table 1. Dipolar Couplings for the α-Linked Galactose of DGDG Dissolved in 30% w/v DMPC/CHAPSO (3:1) at 305 K

	measured (Hz)	corrected (Hz)[a]	predicted (Hz)[b]
H1α−C1α	-782 ± 100	−941	−994
C1α−C2α	$+155 \pm 25$	110	106
C2α−C3α	$\|90\| \pm 25$	−135	−118
C4α−C5α	$+143 \pm 25$	98	106

[a] Corrected values have been adjusted to eliminate the effects of scalar coupling ($^{1}J_{C-C} = 45$ Hz and $^{1}J_{C-H} = 159$ Hz). The signed set that gave the best fit solutions is listed. [b] The predicted values are a representative set from the best fit solution family using a square well model for motional averaging of ϕ_2 and ψ_2 and variable populations for the three minima for ω_2 ($\phi_2 = 80°$; $\psi_2 = 90° \pm 15$; ω_2: 40% −sc, 30% sc, 30% ap). Torsions and description of motional averaging for glycerol backbone and first β-linked galactose were taken from the best fit conformation for MGDG[14] ($\phi_1 = -55°$; $\psi_1 = 210° \pm 60$; $\theta_1 =$ 100% ap; director 15° tilt from long axis of the sn-1 chain; $S_{mol} = 0.62$; $S_{bilayer} = -0.255$). RMSD for the set of predicted couplings listed is 0.009.

Measurement of Dipolar Couplings for the β-Linked Galactose. Resonances from the β-linked galactose were difficult to resolve due to broad line widths and overlap from resonances arising from the α-linked galactose. We were, however, able to extract the C1β−H1β coupling (1420 ± 200 Hz) from a 1D ^{1}H-coupled ^{13}C spectrum. The component line widths are broad, however, making the doublet just barely observable above the noise, as shown in Figure 2c. In addition, the C1β−C2β coupling was resolved in a 2D ^{13}C−^{13}C DQF-COSY (248 ± 50 Hz), facilitated by the well-resolved chemical shift of the C1β resonance. Insufficient resolution prevented measurement of other couplings for the β-linked galactose. Although these two couplings are insufficient for a well-defined description of the β-linked galactose, we were able to take advantage of our recently reported description of the membrane-bound conformation of MGDG.[14]

Since the "core" of DGDG is composed of MGDG, we examined the possibility that the backbone and first sugar of DGDG adopt conformations similar to those of membrane-bound MGDG.[14] Similar CSA offsets for the carbonyl reso-

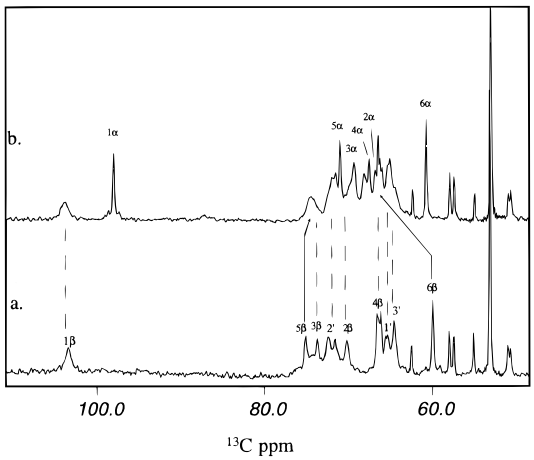

Figure 4. Sugar/glycerol regions of the $^{13}C-^{1}H$ decoupled spectra of (a) 26% ^{13}C MGDG in 30% w/v DMPC/CHAPSO (3:1) and (b) 26% ^{13}C DGDG in 30% w/v DMPC/CHAPSO (3:1).

nances are consistent with similar conformations of the glycerol backbones of MGDG and DGDG. The two couplings measured for β-linked galactose of DGDG are also within experimental error of the analogous couplings in MGDG, suggesting that the two galactose rings have a similar orientation and motion with respect to the membrane. For DGDG, the C1β−H1β and C1β−C2β couplings were 1420 ± 200 and 248 ± 50 Hz, respectively. The analogous couplings in MGDG were 1416 ± 200 and 265 ± 50 Hz. The chemical shifts and line widths for these two residues are also similar. Figure 4 shows the sugar/glycerol region of $^{13}C-^{1}H$ decoupled spectrum of MGDG and DGDG. Most of the sugar/glycerol resonances in MGDG have the same shifts as the analogous sites in DGDG. Only two resonances, C5β and C6β, shift between the two spectra. C5β shifts upfield by 1 ppm, and C6β shifts downfield by 6.5 ppm. These changes can easily be explained, however, by electronic changes due to attachment of another galactose at the C6β position and are also seen in comparing the solution spectra of these two molecules. Thus, the similarity in chemical shifts, dipolar couplings, and line widths between MGDG and the "core" of DGDG supports the idea that it is reasonable to model the backbone and first galactose of DGDG using the conformation and dynamic description of MGDG.

Conformational Analysis. Dipolar couplings measured for the α-linked galactose are subject to motional averaging from several different sources: overall membrane disc motion, rotation about the membrane anchor, oscillations about the torsions linking the backbone to the first galactose, and motions about the α(1−6) interglycosidic torsions. To the extent that we can consider internal motions of the α-linked galactose to be independent of motion in the first galactose and backbone region, the net averaging of dipolar couplings for the α-linked sugar can be considered a simple product of scaling due to disc motion, scaling due to motion of the membrane anchor, scaling due to the β-galactose motions, and scaling due to the α-galactose motions. All orientational and averaging information for the backbone and β-linked sugar was taken from the best fit MGDG solution.[14] The membrane-bound description of the conformation and dynamics of MGDG included an axially symmetric order parameter ($S_{mol} = 0.62$) to account for rotation about the membrane anchor. Furthermore, torsion angle analysis of the linkage between the sugar and the backbone yielded values for the torsion angles, as well as the widths of wells in which the torsions angles were oscillating (footnote *b* of Table 1). After factoring in the reduction of dipolar couplings due the motion of the "core", dipolar couplings for the α-linked

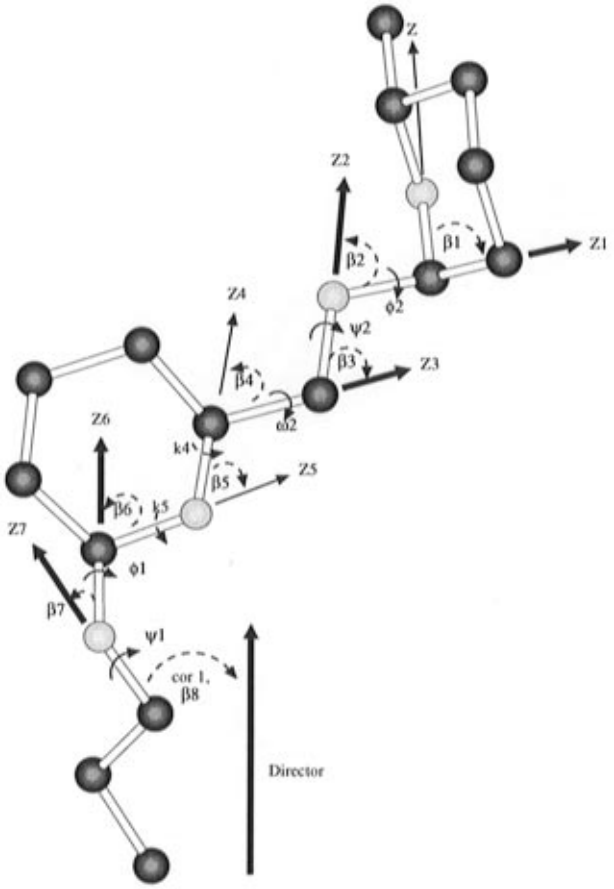

Figure 5. Schematic representation of the rotations performed to fit the dipolar coupling data for DGDG. ϕ_1 = O5β−C1β−O1′β−C1′; ψ_1 = C1β−O1′β−C1′−C2′; θ_1 = O1′β−C1′−C2′−C3′; ϕ_2 = O5α−C1α−O6β−C6β; ψ_2 = C1α−O6β−C6β−C5β; ω_2 = O6β−C6β−C5β−C4β.

galactose were fit by searching over orientations and various levels of motional freedom for the α(1−6) interglycosidic link. Motions about ϕ_2 and ψ_2 are believed to be localized within single broad minima and are modeled using simple square well potentials of different widths.[27] Motional averaging about ω_2 was treated as a weighted average over the three low-energy staggered conformations. Solutions are expressed as centers and well widths for ϕ_2 and ψ_2 and populations of the staggered conformers of ω_2.

A Wigner rotation matrix routine previously applied to simple model glycolipids,[27] as well as the head group of MGDG,[14] was adapted to treat DGDG. The routine simply transforms dipolar interactions from a reference frame (in our case, that of the director) to frames in which *Z* axes are coincident with bonds about which torsional averaging can occur. A schematic of the successive rotations necessary to fully describe the motional averaging is shown in Figure 5. Couplings written in terms of spherical harmonics of the molecular frame for the β-linked sugar closest to the membrane surface were further transformed using Wigner rotation matrices from Z_5 successively to Z_4, Z_3, Z_2, Z_1, and finally to a molecular frame defined with the *Z* axis along C1α−O5α. The bold arrows (Z_1, Z_2, Z_3, Z_6, Z_7, and the director) indicate axes about which averaging is done. The dashed arrows indicate rotations needed to transform from one frame to the next which are fixed by molecular geometry. (Rotations about *Z* axes correspond to Euler α rotations. Rotations from one *Z* axis to the next correspond to Euler β rotations.) A C++ program was written to perform the transformations and fit the dipolar couplings.

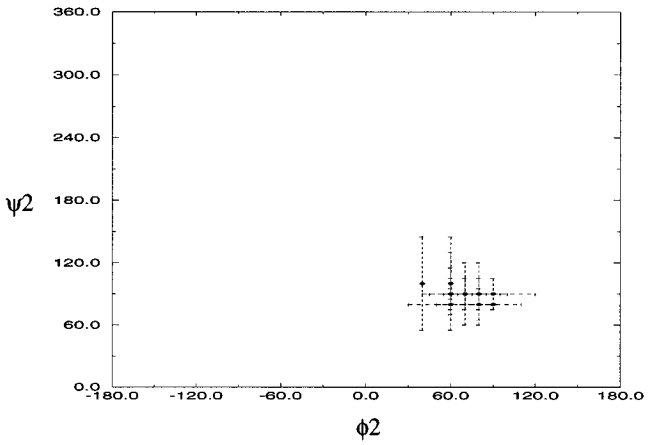

Figure 6. ϕ_2/ψ_2 values for conformations of DGDG which fit the experimental data listed in Table 1 with rmsd less than 0.015. Dotted lines indicate the well widths over which ϕ_2 and ψ_2 are averaged.

Four dipolar couplings were used to fit the conformation of the α-linked galactose (Table 1). Signs for three of the four couplings had been determined. Taking into account both the possible signs for the remaining C2α−C3α coupling, two signed sets were searched. (Acceptable solutions were chosen on the basis of predicted values that were within one-half of a line width of experimental values.) Four solution families were found centered at ($\phi_2 = -100$, $\psi_2 = 60$), ($\phi_2 = 60$, $\psi_2 = 100$), ($\phi_2 = -150$, $\psi_2 = 270$), and ($\phi_2 = 30$, $\psi_2 = 290$). All but ($\phi_2 = 60$, $\psi_2 = 100$) had unfavorable steric contacts between the two galactose residues and fell into high-energy regions of ϕ_2/ψ_2 energy maps (see Discussion). The one family without unfavorable steric contacts, centered at ($\phi_2 = 60$, $\psi_2 = 100$), also had the lowest rmsd (rmsd < 0.015). (For normalization, data were scaled by the maximum expected splitting as reduced by S_{system} before calculation of rmsd.) Figure 6 shows the ϕ_2/ψ_2 values that led to solutions with rmsd < 0.015. They all fall into the ($\phi_2 = 60$, $\psi_2 = 100$) family. The ($\phi = 60$, $\psi = 100$) family has all three conformers about ω_2 approximately equally populated, indicating relatively free rotation about $\omega 2$. The predicted couplings for the best fit solution from this family are listed in Table 1, and a stereo diagram of the best fit conformation is shown in Figure 7.

A somewhat simplified treatment was also used in which we attempted to model motions for each ring in terms of a specific orientation and a single axially symmetric order parameter. This treatment allows a more direct comparison with spin relaxation data to be discussed below. After scaling for system order ($S_{system} = -0.255$) and motion of the glycerol backbone ($S_{mol} = 0.62$), the five dipolar couplings for the β-linked galactose from MGDG were fit to a $S_{\beta ax}$ of 0.8 and an orientation very similar to the best fit solution from torsion angle analysis. A similar approach was used to fit the four dipolar coupling constants measured for the terminal α-linked galactose. After scaling for system order ($S_{system} = -0.255$) and motion of the backbone ($S_{mol} = 0.62$), a $S_{\alpha ax}$ of 0.6 reproduced experimental couplings for an orientation similar to that found using torsion angle analysis.

Relaxation Times. Relaxation times were measured for 26% ^{13}C DGDG embedded in DMPC/CHAPSO under isotropic conditions (20% w/v DMPC/CHAPSO (3:1) at 292 K). The relaxation data measured for the anomeric position of each of the two sugars are listed in Table 2. Relaxation times for other resonances could be measured but were not as clearly resolved and are not reported here. Whereas the NOE and T_2 values are clearly different for the C1α and C1β positions, T_1 values for the two positions are the same within experimental error. Figure 8 is series of spectra from an inversion recovery experiment collected to determine T_1 values. Except for the methylene C6α, C1′, and C3′ sites, the sugar/glycerol resonances recover at very similar rates, passing through zero at a time which is within 20% of that for the anomerics.

Relaxation rates give information about the rotational fluctuations of the ^{13}C−^{1}H bond vectors with respect to the external magnetic field. The following relationships for the relaxation of methine carbons by a single ^{13}C−^{1}H dipolar interaction adequately serve for our relaxation analysis.[42,43] Use of these approximate expressions is justified by the large γ for a proton and the short internuclear distance for the directly bonded pair.

$$\frac{1}{T_1} = \frac{\hbar^2 \gamma_H^{\,2} \gamma_C^{\,2}}{3r^6}[J(\omega_C - \omega_H) + 3J(\omega_C) + 6J(\omega_C + \omega_H)] \quad (3)$$

$$\mathrm{NOE} = 1 + \frac{\gamma_H[6J(\omega_C + \omega_H) - J(\omega_C - \omega_H)]}{\gamma_C[J(\omega_C - \omega_H) + 3J(\omega_C) + 6J(\omega_C + \omega_H)]} \quad (4)$$

$$\frac{1}{T_2} = \frac{\hbar^2 \gamma_H^{\,2} \gamma_C^{\,2}}{6r^6}[4J(0) + J(\omega_C - \omega_H) + 3J(\omega_C) + 6J(\omega_H) + 6J(\omega_C + \omega_H)] \quad (5)$$

γ_H and γ_C are the gyromagnetic ratios for ^{1}H and ^{13}C, $\hbar$ is Planck's constant divided by 2π, r is the distance between the two nuclei, and ω_H and ω_C are the Larmor frequencies for ^{1}H and ^{13}C. $J(\omega)$ are the spectral density functions for the associated carbon−proton bond motions. The dynamic information in the relaxation parameters enters through their dependence on $J(\omega)$.

The information obtained from T_1, T_2, and NOE measurements is not sufficient to characterize the bond dynamics without first making some assumptions about the form of $J(\omega)$ itself. An assortment of motional models for dynamics of XH bonds with preassumed analytical dependencies on certain parameters have been presented in the literature.[42,44,45] An alternative to assumption of a specific motional model has been presented by Lipari and Szabo.[45] Their approach makes a minimum of assumptions about XH vector dynamics and introduces a generalized order parameter that can later be interpreted in terms of a variety of more specific motional models. If the molecular dynamics are described by only two different correlation times, τ_m for the overall motions and τ_i for the internal motions, spectral densities can be expressed in the following form:[45]

$$J(\omega) = S^2 \frac{\tau_m}{1 + \omega^2 \tau_m^{\,2}} + (1 - S^2) \frac{\tau_e}{1 + \omega^2 \tau_e^{\,2}} \quad (6)$$

where S^2 is a generalized square order parameter measuring the degree of spatial restriction of the internal motion and $\tau_e^{-1} = \tau_m^{-1} + \tau_i^{-1}$. This expression is exact when the internal (but not the overall) motions are in the extreme narrowing limit.[45]

For certain limiting cases, the form of eq 6 can be understood. $(1 - S^2)$ measures the amplitude of motion due to internal dynamics. When internal motions are fast compared to overall motion, $\tau_i \ll \tau_m$, the internal motions average interactions to

(42) Richarz, R.; Nagayama, K.; Wuthrich, K. *Biochemistry* **1980**, *19*, 5189−5196.
(43) Abragam, A. *Principles of Nuclear Magnetism*; Clarendon Press: Oxford, U.K., 1961.
(44) Woessner, D. *J. Chem. Phys.* **1962**, *36*, 1−4.
(45) Lipari, G.; Szabo, A. *J. Am. Chem. Soc.* **1982**, *104*, 4546−4559.
(46) Chung, J.; Prestegard, J. *J. Phys. Chem.* **1993**, *97*, 9837−9843.
(47) Carrington, A.; McLachlan, A. *Introduction to Magnetic Resonance*; Harper & Row: New York, 1967.

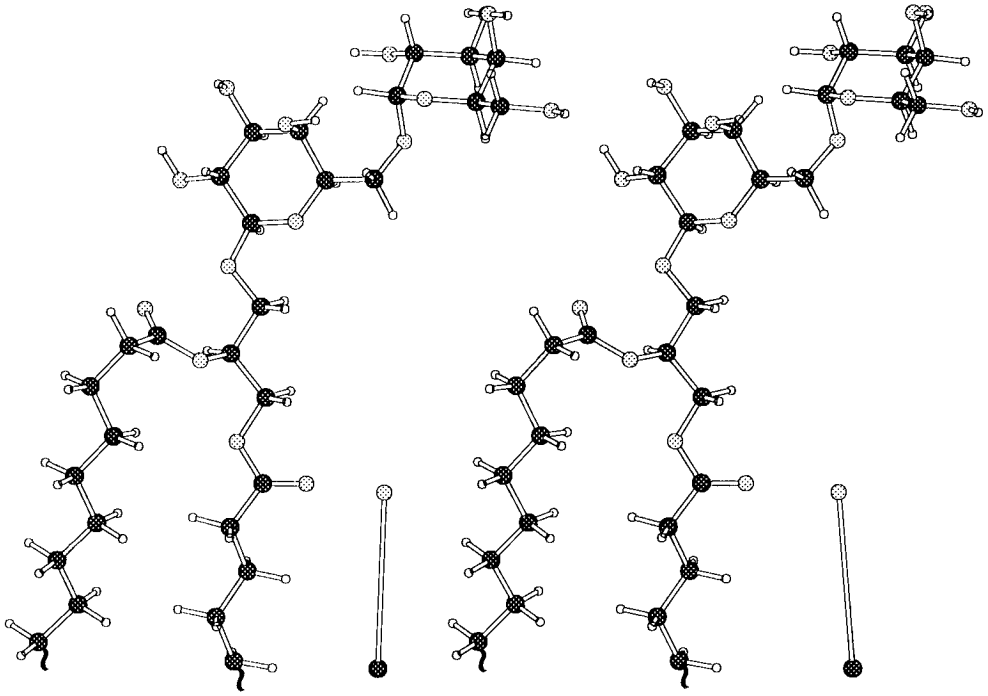

Figure 7. Stereo diagram of the best fit membrane-bound conformation for DGDG as described in footnote *b* of Table 1. Although all three staggered populations of ω_2 are populated in the solution, ω_2 (O6β−C6β−C5β−C4β) is set to −60° in the structure shown. Including the spectral parameters used to fit the conformation of MGDG (utilized in modeling the glycerol backbone and first β-linked sugar), the membrane-bound conformation of DGDG shown is consistent with 15 different spectral parameters (13 dipolar couplings and two CSA offsets).

Table 2. Relaxation Data for the Anomeric Carbons of 26% ^{13}C DGDG in 20% w/v DMPC/CHAPSO (3:1) at 292 K

	C1β		C1α	
	measd	calcd	measd	calcd
NOE	1.3 ± 0.1	1.7	1.9 ± 0.1	2.4
T_2	$(3.3 \pm 0.02) \times 10^{-3}$ s	3.3×10^{-3} s	$(8.1 \pm 0.02) \times 10^{-3}$ s	8.1×10^{-3} s
T_1	$(4.4 \pm 0.3) \times 10^{-1}$ s	4.0×10^{-1} s	$(4.2 \pm 0.3) \times 10^{-1}$ s	4.4×10^{-1} s

the point where only the nonaveraged part, S^2, is effectively modulated by overall motion. Hence, the scaling of two motional functions by S^2 and $(1 - S^2)$ respectively.

Direct application of eq 6 is appropriate for the first β-linked sugar. It is also possible to extend the above analysis to interpretation of dynamics of the second α-linked sugar, assuming the motions of the second sugar are superimposed on motions that the β sugar executes. The resulting equation is as follows:

$$J(\omega) = S_\alpha^2\left(S_\beta^2 \frac{\tau_m}{1+\omega^2\tau_m^2} + (1-S_\beta^2)\frac{\tau_\beta}{1+\omega^2\tau_\beta^2}\right) + (1-S_\alpha^2)\frac{\tau_\alpha}{1+\omega^2\tau_\alpha^2} \quad (7)$$

where S_α^2 and τ_α describe the internal motions of α-galactose and S_β^2 and τ_β describe the internal motions of the β-galactose. ($\tau_\beta^{-1} = \tau_m^{-1} + \tau_{\beta i}^{-1}$ and $\tau_\alpha^{-1} = \tau_m^{-1} + \tau_{\beta i}^{-1} + \tau_{\alpha i}^{-1}$) The relaxation parameters were adjusted using the Levenburg−Marquardt algorithm to perform a nonlinear least squares fit to reproduce the observed relaxation data.

Our first step in analyzing measured relaxation times was to fit the relaxation data for C1β to a τ_m for the overall motion of the discs and S_β^2 and τ_β for internal motion of the first sugar. Relaxation data for C1α were then fit to a S_α^2 and τ_α for internal motion of the terminal sugar using the previously calculated τ_m, S_β^2, and τ_β. The procedure was then iterated constraining $\tau_\beta \geq \tau_\alpha$. The resultant values for τ_m, S_β^2, and τ_β are 133 ns, 0.66, and 0.12 ns, and those for S_α^2 and τ_α are 0.40 and 0.12 ns. The best fit calculated values for the NOE, T_2, and T_1 are included in Table 2. Agreement is good except for the tendency for calculated NOEs to be slightly large. This may be the result of neglecting non-^{1}H−^{13}C dipolar contributions to ^{13}C relaxation. The similarity of τ_β and τ_α would seem problematic since eq 7 was justified on the basis of superimposing a faster motion for the terminal sugar on a slower motion for the internal sugar. However, it is noteworthy that eq 7 goes cleanly to eq 6 with $S^2 = S_\alpha^2 S_\beta^2$ in the limit of $\tau_\alpha = \tau_\beta$, so the product $S_\alpha^2 S_\beta^2$ is always well-determined. The separability of $S_\alpha^2 S_\beta^2$ may be somewhat suspect.

Discussion

From the results presented above, we have been able to derive a detailed description of both the conformation and dynamics of the carbohydrate head group of membrane-bound DGDG. The digalactosyl head group is extended away from the membrane surface. While there is relatively restricted motion about the β-linkage between the backbone and the first sugar, motion about the α-linkage between the two sugars is considerable.

The proposed structure and mobility can be compared with related data in the literature. We have discussed the membrane-bound properties of the glycerol backbone and the β-linked sugar in a previous publication[14] and will focus on the α(1−6) intergalactose linkage here. The glycosidic torsion ϕ_2 is 80° (with no motional averaging about this torsion) in our best fit solution for DGDG. This is consistent with well-defined torsion

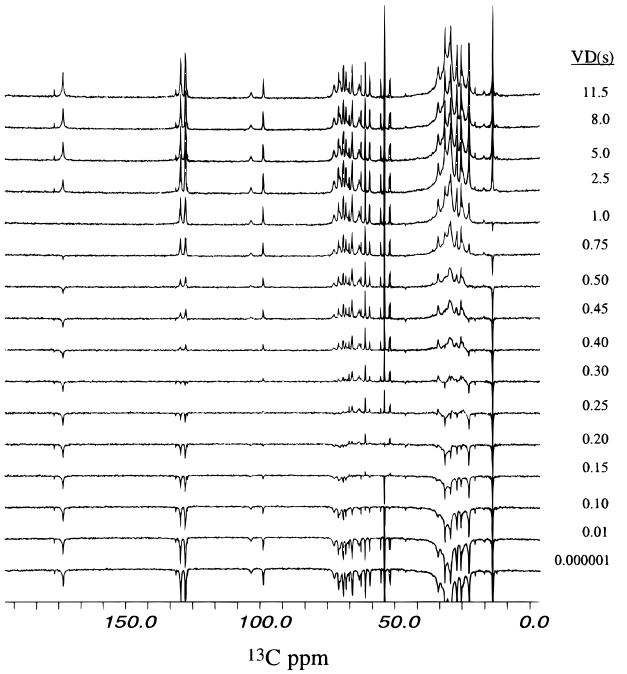

Figure 8. Inversion recovery experiment (180−τ−90) for 26% ^{13}C DGDG in 20% w/v DMPC/CHAPSO (3:1) at 293 K. The τ values varied between experiments and are listed as variable delay (VD).

angle homologies for ϕ angles occurring in α(1−6) linkages in published x-ray crystal structures[48] which indicate a distinct preference for +sc for ϕ(O5−C1−O1−C6′). The best fit solution also involves a +sc conformation for ψ_2 but allows for moderate motion about this position ($\psi_2 = 90 \pm 15$). Furthermore, the best fit solution involves approximately equal populations of each of the staggered conformations of ω_2 (i.e., +sc, −sc, and ap are all populated). Torsion angle distributions for ψ and ω in α(1−6) linkages in published X-ray crystal structures[48] are somewhat broader than those observed for for ϕ torsions in (1−6) linkages (ψ(+sc, ap) and ω(+sc, −sc)). It is noteworthy that the ϕ_2/ψ_2 conformation in our best fit conformation extends the terminal sugar away from the first galactose and membrane surface, allowing nearly unhindered rotation about ω_2. This results in a high degree of flexibility. Several NMR studies[15,49,50] and molecular modeling studies[51,52] have also concluded that (1−6) glycosidically linked branches in complex carbohydrates exhibit considerable flexibility. It has been suggested that (1−6) linkages provide oligosaccharides with the necessary flexibility to adopt conformations which result in strong interactions with proteins.[52]

Studying molecules at membrane surfaces has been an experimental challenge, and most previous studies have focused on glycolipids with single residue head groups[8,10,16−18] or isolated sites in more complex glycolipid head groups.[26,53] A few studies have treated more complex systems. Jarrell and co-workers studied the disaccharide head group of a lactose-containing lipid relative to the surface of bilayer membranes using ^{2}H NMR to measure quadrupole splittings and spin−lattice relaxation times.[54] Like our results for DGDG, their data were consistent with a glycolipid head group that extends away from the membrane surface. However, unlike the flexibility of the α-galactose of DGDG, they found little motion about the disaccharide (1−4) linkage of their glycolipid.

Whereas the dipolar coupling information yields a qualitative indication of amplitudes of motion about the (1−6) linkage, time scales of the motional averaging must come from other sources. In the past, relaxation studies on small carbohydrates in solution have been plagued by the complication that internal motions were on a time scale close to that of the overall molecular tumbling. This inhibits their separation on the basis of time scales.[55] Here, however, the slow tumbling of the DMPC/CHAPSO assemblies provides a slow overall tumbling which allows the resolution of the much faster internal motions of the flexible glycosidic linkages.

The time characterizing overall tumbling of lipid molecules attached to DMPC/CHAPSO micelles in our relaxation analysis is τ_m which has a value of 133 ns. This might be compared to a tumbling time for a micelle of the size estimated from pulsed field gradient spin echo techniques.[46] Using the Stokes−Einstein equation,[47] the correlation time for an isolated spherical micelle of the same volume in pure water would be 420 ns. The difference very likely reflects the presence of some additional slow motions of the constituent lipid backbones within the micelle matrix.

The times characterizing motions of the individual sugar residues relative to the lipid backbone are given by τ_β and τ_α (0.12 ns). Given that the best fit values depart from the $\tau_\alpha < \tau_\beta$ limits of our model, these must be interpreted with caution. However, it is appropriate to note that the motions are predicted to be quite rapid. The rates are not unreasonable for wobble within ϕ, ψ, ω, and θ torsion wells.

It is possible to check for consistency between the model fitting dipolar coupling data and the model fitting relaxation rates by comparison of the axially symmetric order parameters, $S_{\beta ax}$ and $S_{\alpha ax}$, from dipolar coupling data and generalized order parameters S_β and S_α from spin relaxation studies. Lipari and Szabo call S a generalized order parameter because it reduces to the usual order parameter S_{ax} in certain limits.[45] In the special case that motion is azimuthally symmetric about an axis

$$S = \left\langle \frac{3\cos\theta^2 - 1}{2} \right\rangle = S_{ax} \qquad (8)$$

where θ is the angle between the internuclear vector and the symmetry axis. As detailed in the Results, $S_{\beta ax}$ for the β-linked sugar is 0.8. This is very close to the S_β which fit the relaxation data; $S_\beta = \sqrt{S_\beta{}^2} = 0.81$. $S_{\alpha ax}$ for the α-linked sugar is 0.6, which includes all motional averaging above the backbone (i.e., both averaging about the backbone β-galactose link, as well as the α(1−6) interglycosidic link). This is again close to the product of the generalized order parameters from the relaxation data ($S_\alpha S_\beta = 0.51$).

The concept of an order parameter resulting from the incomplete averaging of second-rank tensor interactions plays a central role in interpretation of several magnetic resonance methods, including electron spin resonance and deuterium NMR. Efforts have been made to relate order parameters determined by the various techniques with variable success.[56] In cases of disagreement, the sensitivity of methods to different time scales has often been cited. In our case, the level of agreement between relaxation derived and orientation derived order parameters is quite good.

(48) Jeffrey, G. *Acta Crystallogr.* **1990**, *B46*, 89−103.
(49) Brisson, J.; Carver, J. *Biochemistry* **1983**, *22*, 3680−3686.
(50) Ohrui, H.; Nishida, Y.; Watanabe, M.; Hori, H.; Meguro, H., *Tetrahedron Lett.* **1985**, *26*, 3251−3254.
(51) Qasba, P.; Balaji, P.; Rao, V. *Glycobiology* **1994**, *4*, 805−815.
(52) Stuike-Prill, R.; Meyer, B. *Eur. J. Biochem.* **1990**, *194*, 903−919.
(53) Aubin, Y.; Ito, Y.; Paulson, J.; Prestegard, J. *Biochemistry* **1993**, *32*, 13405−13413.
(54) Renou, J.; Giziiewicz, J.; Smith, I.; Jarrell, H. *Biochemistry* **1989**, *28*, 1804−1814.
(55) Bush, C. *Biophys. J.* **1994**, *66*, 1267−1273.
(56) Petersen , N.; Chan, S. *Biochemistry* **1977**, *16*, 2657−2667.

Another recent study used the anchoring effect of micelles to allow detection of conformational fluctuations of a complex glycolipid head group.[22] Poppe and co-workers anchored the non-isotopically labeled ganglioside GD1a to perdeuterated dodecylphosphocholine (DPC) micelles and used ^{1}H-detected ^{13}C relaxation times to describe the flexibility of a terminal trisaccharide moiety with respect to the core of the glycolipid which consists of three other sugars and a cerebroside anchor. They used relaxation parameters for the core (assuming $S^2 = 1$ and $\tau_i = 0$) to solve for a τ_m, which was then used for analysis of τ_i and S^2 for the terminal trisaccharide. Their micelles were much smaller than the large DMPC assemblies used here, and their τ_m was 2.8 ns. S was 0.74 and τ_i was 0.34 ns for the terminal moiety. The flexible linkage under study was a $\beta(1-3)$ link which might be predicted to exhibit less flexibility than the $\alpha(1-6)$ linkage in DGDG which has an additional degree of freedom.

A systematic way to evaluate observed conformational preferences of glycolipids is to calculate energy maps as a function of glycosidic torsions. Potential energy maps were calculated for the $\alpha(1-6)$ linkages of DGDG as a function of ϕ_2 and ψ_2, one for each of the staggered conformations of ω_2 (see Figure 9). The darkest shaded area is the highest energy region and is at least 13 kcal/mol higher in energy than the energy minima. There is a strip of energy minima along ϕ_2 = sc, which is consistent with crystal structures of α-glycosides.[48] Minima for both ψ_2 and ω_2 occur at all three staggered conformations. This is in close agreement with a recent molecular dynamics study of an $\alpha(1-6)$ linkage.[51] The global minimum is located at $\phi_2 = 80/\psi_2 = 60/\omega_2$ = sc and is marked with an ×. The best fit membrane conformation (indicated with a dashed box) includes population of the global minimum as well as local minima at ϕ_2/ψ_2 = sc/sc for the other two staggered ω_2 conformations.

The maps shown in Figure 9 include a membrane interaction energy. This energy is essentially a solvation term dependent on an effective dielectric constant that is low inside the membrane and high well outside the surface.[28] A set of potential energy maps analogous to Figure 9, but without a membrane interaction energy, was also calculated for DGDG (not shown). The solution and membrane maps for the interglycosidic linkage of DGDG are very similar in terms of the location, depth, and width of energy minima. In fact, they share a global minimum. The absolute values of the energies without the membrane interaction term are, however, 80−90 kcal/mol higher in energy. This behavior contrasts with that observed for MGDG,[14] where the membrane interaction energy stabilized particular regions of the map, leading to a different global minimum in solution and membrane maps. In addition, for MGDG, additions to energies from the membrane interaction were on the order of just a few kilocalories per mole. The membrane interaction term makes larger contributions for DGDG because the membrane energy scales up with the total number of dipoles and is accentuated by having the second sugar in a very high dielectric region. However, the difference, not the absolute magnitude of the energies, serves to preferentially stabilize some minima over others. For MGDG, the range of membrane energies was 5 kcal/mol, whereas for DGDG, the range is just 3 kcal/mol and the membrane energies have a minimal effect on the energy profile. This can be explained by the fact that the linkage

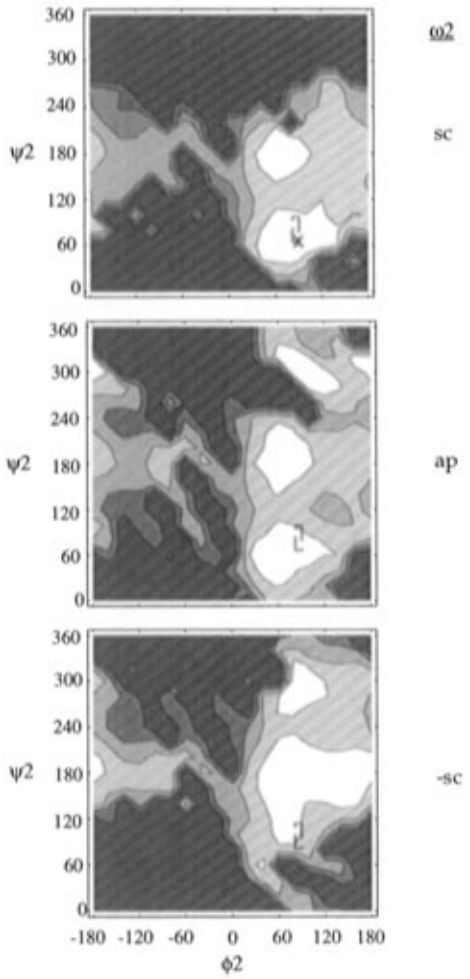

Figure 9. Potential energy maps for the $\alpha(1-6)$ interglycosidic linkage of membrane-bound DGDG as a function of ϕ_2, ψ_2, and ω_2. The dashed rectangle encompasses conformations within the range of motion for the best fit membrane-bound solution [global minimum (×)]. Contours are 3.5 kcal/mol apart. Darkest shaded area is the highest energy region and is at least 13 kcal/mol higher in energy than ×.

modeled in MGDG occurs close to the membrane interface in a region where the dielectric variation is steep. On the other hand, the second α-linked galactose of DGDG is extended by the first galactose out into the aqueous region where variations in dielectric constant with motions about ϕ_2, ψ_2, and ω_2 are minimal. Thus, it appears that, while membrane effects may be important in producing preferred extended conformations linkages in glycolipids occurring close to the membrane interface,[14] explicit inclusion of membrane effects may be unnecessary for sugar residues that are removed from the membrane surface.

Thus, we have been able to integrate both dipolar coupling and ^{13}C relaxation data into a detailed description of the membrane-bound conformation and dynamics of an abundant, naturally occurring complex glycolipid. The NMR studies of membrane fragments presented here prove to be a useful approach to experimentally determining membrane-bound structures of uniformly ^{13}C-labeled molecules.

JA952971Y